

Chapter 14

Equatorial Processes

Equatorial processes are important for understanding the influence of the ocean on the atmosphere and the interannual fluctuations in global weather patterns. The sun warms the vast expanses of the tropical Pacific and Indian Oceans, evaporating water. When the water condenses as rain it releases so much heat that these areas are the primary engine driving the atmospheric circulation (Figure 14.1). Rainfall over extensive areas exceeds three meters per year, and some oceanic regions receive more than five meters of rain per year. To put the numbers in perspective, five meters of rain per year releases on average 400 W/m^2 of heat to the atmosphere. Equatorial currents modulate the air-sea interactions, especially through the phenomenon known as El Niño, with global consequences. We describe here first the basic equatorial processes, then the year-to-year variability of the processes and the influence of the variability on weather patterns.

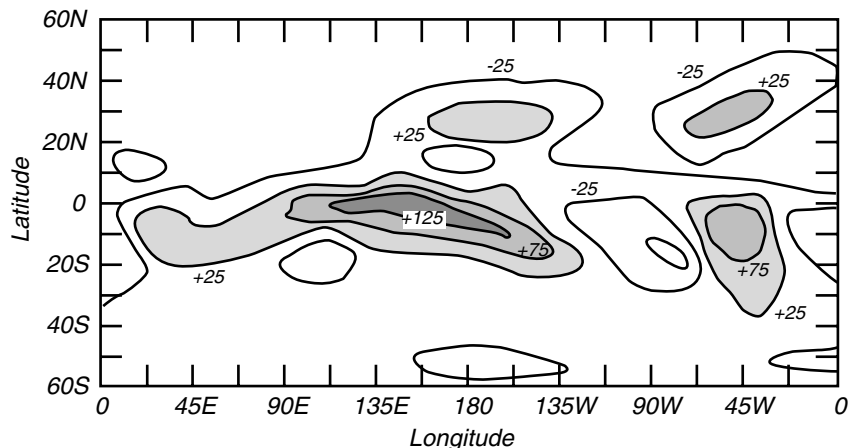


Figure 14.1 Average diabatic heating due to rain, absorbed solar and infrared radiation and between 700 and 50 mb in the atmosphere during December, January and February calculated from ECMWF data for 1983–1989. Most of the heating is due to the release of latent heat by rain (From Webster, 1992).

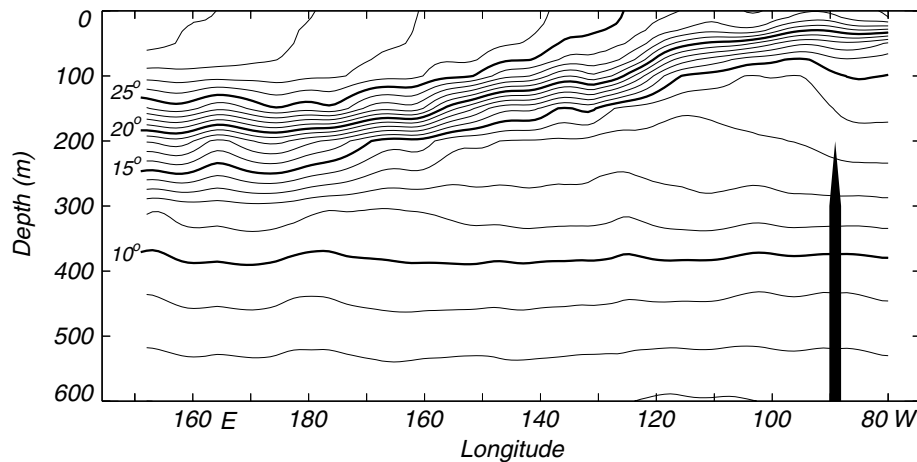


Figure 14.2 The mean, upper-ocean, thermal structure along the equator in the Pacific from north of New Guinea to Ecuador calculated from data in Levitus (1982).

14.1 Equatorial Processes

The tropical regions are characterized by a thin, permanent, shallow layer of warm water over deeper, colder water. In this respect, the vertical stratification is similar to the summer stratification at higher latitudes. Surface waters are hottest in the west (Figure 6.3) in the great Pacific warm pool. The mixed layer is deep in the west and very shallow in the east (Figure 14.2).

The shallow thermocline has important consequences. The southeast trade winds blow along the equator (Figure 4.2) although they tend to be strongest in the east. North of the equator, Ekman transport is northward; south of the equator it is southward. The divergence of the Ekman flow causes upwelling on the equator. In the west, the upwelled water is warm. But in the east the upwelled water is cold because the thermocline is so shallow. This leads to a cold tongue of water at the sea surface extending from South America to near the dateline (Figure 6.3).

Surface temperature in the east is a balance among four processes:

1. The strength of the upwelling, which is determined by the westward component of the wind.
2. The speed of westward currents which carry cold water from the coast of Peru and Ecuador.
3. North-south mixing with warmer waters on either side of the equator.
4. Heat fluxes through the sea surface along the equator.

The east-west temperature gradient on the equator drives a zonal circulation in the atmosphere, the Walker circulation. Thunderstorms over the warm pool carry air upward, and sinking air in the east feeds the return flow at the surface. Variations in the temperature gradient influences the Walker circulation, which, in turn, influences the gradient. The feedback can lead to an instability, the El Niño-Southern Oscillation (ENSO) discussed in the next section.

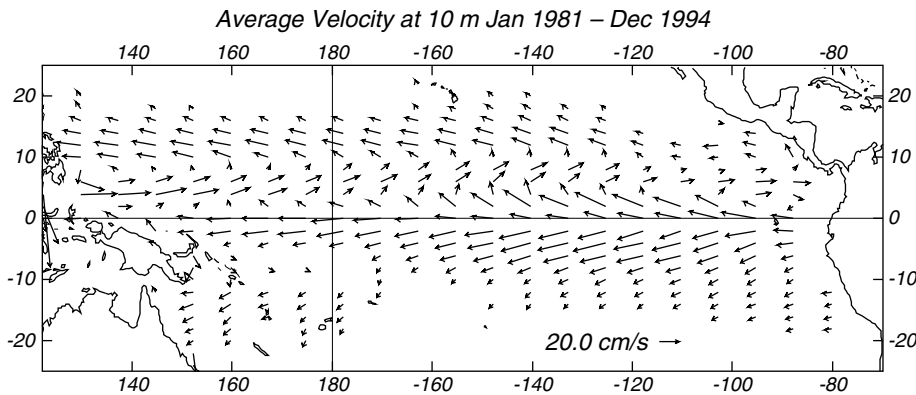


Figure 14.3 Average currents at 10 m calculated from the Modular Ocean Model driven by observed winds and mean heat fluxes from 1981 to 1994. The model, operated by the NOAA National Centers for Environmental Prediction, assimilates observed surface and subsurface temperatures (From Behringer, Ji, and Leetmaa, 1998).

Surface Currents The strong stratification confines the wind-driven circulation to the mixed layer and upper thermocline. Sverdrup's theory and Munk's extension, described in §11.1 and §11.3, explain the surface currents in the tropical Atlantic, Pacific, and Indian Oceans. The currents include (Figure 14.3):

1. The North Equatorial Countercurrent between 3°N and 10°N , which flows eastward with a typical surface speed of 50 cm/s. The current is centered on the band of weak winds, the *doldrums*, that exist at the latitude where the north and south trade winds converge, the *tropical convergence zone*.
2. The North and South Equatorial Currents which flow westward in the zonal band on either side of the countercurrent. The currents are shallow, less than 200 m deep. The northern current is weak, with a speed less than roughly 20 cm/s. The southern current has a maximum speed of around 100 cm/s, in the band between 3°N and the equator.

The currents in the Atlantic are similar to those in the Pacific because the trade winds in that ocean also converge near 5° – 10°N . The South Equatorial Current in the Atlantic continues northwest along the coast of Brazil, where it is known as the North Brazil Current. In the Indian Ocean, the doldrums occur in the southern hemisphere and only during the northern-hemisphere winter. In the northern hemisphere, the currents reverse with the monsoon winds.

There is, however, much more to the story of equatorial currents.

Equatorial Undercurrent: Observations Just a few meters below the surface on the equator is a strong eastward flowing current, the Equatorial Undercurrent, the last major oceanic current to be discovered. Here's the story:

In September 1951, aboard the U.S. Fish and Wildlife Service research vessel long-line fishing on the equator south of Hawaii, it was noticed that the subsurface gear drifted steadily to the east. The next year Cromwell,

in company with Montgomery and Stroup, led an expedition to investigate the vertical distribution of horizontal velocity at the equator. Using floating drogues at the surface and at various depths, they were able to establish the presence, near the equator in the central Pacific, of a strong, narrow eastward current in the lower part of the surface layer and the upper part of the thermocline (Cromwell, *et. al.*, 1954). A few years later the Scripps *Eastropic* Expedition, under Cromwell's leadership, found the current extended toward the east nearly to the Galapagos Islands but was not present between those islands and the South American continent.

The current is remarkable in that, even though comparable in transport to the Florida Current, its presence was unsuspected ten years ago; even now, neither the source nor the ultimate fate of its waters has been established. No theory of oceanic circulation predicted its existence, and only now are such theories being modified to account for the important features of its flow.—Warren S. Wooster (1960).

Evidence for an Equatorial Undercurrent had been noted by Buchanan, Krümmel, Puls, and others in the Atlantic (Neumann, 1960).

However, no attention was paid to them. Other earlier hints regarding this undercurrent were mentioned by Matthäus (1969). Thus the old experience becomes even more obvious which says that discoveries not attracting the attention of contemporaries simply do not exist.—Dietrich *et al.* (1980).

Bob Arthur (1960) summarized the major aspects of the flow:

1. Surface flow may be directed westward at speeds of 25–75 cm/s;
2. Current reverses at a depth of from 20 to 40 m;
3. Eastward undercurrent extends to a depth of 400 meters with a transport of as much as $30 \text{ Sv} = 30 \times 10^6 \text{ m}^3/\text{s}$;
4. Core of maximum eastward velocity (0.50–1.50 m/s) rises from a depth of 100 m at 140°W to 40 m at 98°W , then dips down;
5. Undercurrent appears to be symmetrical about the equator and becomes much thinner and weaker at 2°N and 2°S .

In essence, the Pacific Equatorial Undercurrent is a ribbon with dimensions of $0.2 \text{ km} \times 300 \text{ km} \times 13,000 \text{ km}$ (Figure 14.4).

Equatorial Undercurrent: Theory Although we do not yet have a complete theory for the undercurrent, we do have a clear understanding of some of the more important processes at work in the equatorial regions. Pedlosky(1996), in his excellent chapter on Equatorial Dynamics of the Thermocline: The Equatorial Undercurrent, points out that the basic dynamical balances we have used in mid latitudes break down near or on the equator.

Near the equator:

1. The Coriolis parameter becomes very small, going to zero at the equator:

$$f = 2\Omega \sin \varphi = \beta y \approx 2\Omega \varphi \quad (14.1)$$

where φ is latitude, $\beta = \partial f / \partial y \approx 2\Omega / R$ near the equator, and $y = R\varphi$.

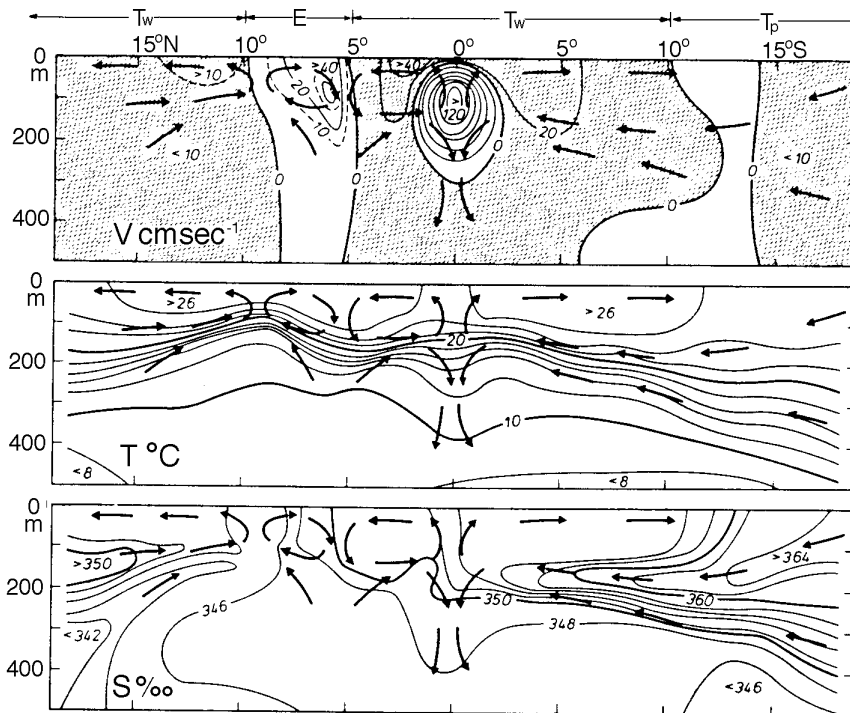


Figure 14.4 Cross Section of the Equatorial Undercurrent in the Pacific. Stippled areas are westward flowing. Arrows give transverse flow. (After Dietrich, 1970).

2. Planetary vorticity f is also small, and the advection of relative vorticity cannot be neglected. Thus the Sverdrup balance (11.7) must be modified.
3. The geostrophic and vorticity balances fail when the meridional distance L to the equator is $O(\sqrt{U/\beta})$, where $\beta = \partial f/\partial y$. If $U = 1$ m/s, then $L = 200$ km or 2° of latitude. Lagerloeff et al (1999), using measured currents, show that currents near the equator can be described by the geostrophic balance for $|\varphi| > 2.2^\circ$. They also show that flow closer to the equator can be described using a β -plane approximation $f = \beta y$.
4. The geostrophic balance for *zonal* currents works so well near the equator because f and $\partial\zeta/\partial y \rightarrow 0$ as $\varphi \rightarrow 0$, where ζ is sea surface topography.

The upwelled water along the equator produced by Ekman pumping is not part of a two-dimensional flow in a north-south, meridional plane. Instead, the flow is three-dimensional. The water tends to flow along the contours of constant density (isopycnal surfaces), which are close to the lines of constant temperature in Figure 14.2. Cold water enters the undercurrent in the far west Pacific, it moves eastward along the equator, and as it does it moves closer to the surface. Note, for example, that the 25° isotherm enters the undercurrent at a depth near 125 m in the western Pacific at 170°E and eventually reaches the surface at 125°W in the eastern Pacific.

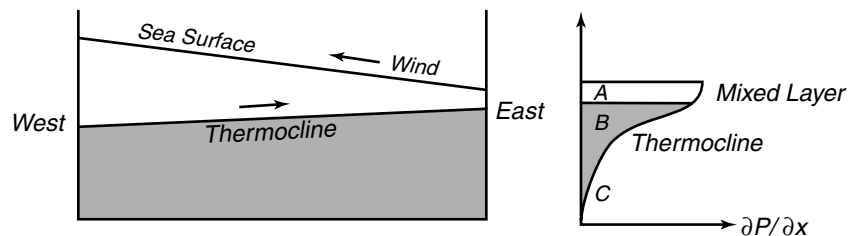


Figure 14.5 **Left:** Cross-sectional sketch of the thermocline and sea-surface topography along the equator. **Right:** Eastward pressure gradient in the central Pacific caused by the density structure at left.

The meridional geostrophic balance near the equator gives the speed of the zonal currents, but it does not explain what drives the undercurrent. A very simplified theory for the undercurrent is based on a balance of zonal pressure gradients along the equator. Wind stress pushes water westward, producing the deep thermocline and warm pool in the west. The deepening of the thermocline causes the sea-surface topography ζ to be higher in the west, assuming that flow below the thermocline is weak. Thus there is an eastward pressure gradient along the equator in the surface layers to a depth of a few hundred meters. The eastward pressure gradient at the surface is balanced by the wind stress T_x , (layer A in Figure 14.5), so $T_x = -\partial p/\partial x$.

Below a few tens of meters in layer B, the influence of the wind stress is small, and the pressure gradient is unbalanced, leading to an accelerated flow toward the east, the equatorial undercurrent. Within this layer, the flow accelerates until the pressure gradient is balanced by frictional forces which tend to slow the current. At depths below a few hundred meters in layer C, the eastward pressure gradient is too weak to produce a current, $\partial p/\partial x \approx 0$.

Coriolis forces keep the equatorial undercurrent centered on the equator. If the flow strays northward, the Coriolis force deflects the current southward. The opposite occurs if the flow strays southward.

14.2 Variable Equatorial Circulation: El Niño/La Niña

The trades are remarkably steady, but they do vary from month to month and year to year, especially in the western Pacific. One important source of variability are Madden-Julian waves in the atmosphere (McPhaden, 1999). If the trades in the west weaken or even reverse, the air-sea system in the equatorial regions can be thrown into another state called El Niño. This disruption of the equatorial system in the Pacific disrupts weather around the globe.

Although the modern meaning of the term El Niño denotes a disruption of the entire equatorial system in the Pacific, the term has been used in the past to describe several very different processes. This causes a lot of confusion. To reduce the confusion, let's learn a little history.

A Little History Many years ago, way back in the 19th century, the term was applied to conditions off the coast of Peru. The following quote comes from the introduction to Philander's (1990) excellent book *El Niño, La Niña, and the Southern Oscillation*:

In the year 1891, Señor Dr. Luis Carranza of the Lima Geographical Society, contributed a small article to the Bulletin of that Society, calling attention to the fact that a counter-current flowing from north to south had been observed between the ports of Paita and Pacasmayo.

The Paita sailors, who frequently navigate along the coast in small craft, either to the north or the south of that port, name this counter-current the current of “El Niño” (the Child Jesus) because it has been observed to appear immediately after Christmas.

As this counter-current has been noticed on different occasions, and its appearance along the Peruvian coast has been concurrent with rains in latitudes where it seldom if ever rains to any great extent, I wish, on the present occasion, to call the attention of the distinguished geographers here assembled to this phenomenon, which exercises, undoubtably, a very great influence over the climatatic conditions of that part of the world.—Señor Frederico Alfonso Pezet’s address to the Sixth International Geographical Congress in Lima, Peru 1895.

The Peruvians noticed that in some years the El Niño current was stronger than normal, it penetrated further south, and it is associated with heavy rains in Peru. This occurred in 1891 when (again quoting from Philander’s book)

... it was then seen that, whereas nearly every summer here and there there is a trace of the current along the coast, in that year it was so visible, and its effects were so palpable by the fact that large dead alligators and trunks of trees were borne down to Pacasmayo from the north, and that the whole temperature of that portion of Peru suffered such a change owing to the hot current that bathed the coast. ... —Señor Frederico Alfonso Pezet.

... the sea is full of wonders, the land even more so. First of all the desert becomes a garden The soil is soaked by the heavy downpour, and within a few weeks the whole country is covered by abundant pasture. The natural increase of flocks is practically doubled and cotton can be grown in places where in other years vegetation seems impossible.—From Mr. S.M. Scott & Mr. H. Twiddle quoted from Murphy (1926).

The El Niño of 1957 was even more exceptional. So much so that it attracted the attention of meteorologists and oceanographers throughout the Pacific basin.

By the fall of 1957, the coral ring of Canton Island, in the memory of man ever bleak and dry, was lush with the seedlings of countless tropical trees and vines.

One is inclined to select the events of this isolated atoll as epitomizing the year, for even here, on the remote edges of the Pacific, vast concerted shifts in the oceans and atmosphere had wrought dramatic change.

Elsewhere about the Pacific it also was common knowledge that the year had been one of extraordinary climatic events. Hawaii had its first recorded typhoon; the seabird-killing *El Niño* visited the Peruvian coast; the ice went out of Point Barrow at the earliest time in history; and on the Pacific’s western rim, the tropical rainy season lingered six weeks beyond its appointed term—Sette and Isaacs (1960).

Just months after the event, in 1958, a distinguished group of oceanographers and meteorologists assembled in Rancho Santa Fe, California to try to understand the *Changing Pacific Ocean in 1957 and 1958*. There, for perhaps the first time, they began the synthesis of meteorological events with oceanographic observations leading to our present understanding of El Niño.

While oceanographers had been mostly concerned with the eastern equatorial Pacific and El Niño, meteorologists had been mostly concerned with the western tropical Pacific, the tropical Indian Ocean, and what they called the Southern Oscillation. Hildebrandsson, the Lockyers, and Sir Gilbert Walker noticed in the early decades of the 20th century that pressure fluctuations throughout that region are highly correlated with pressure fluctuations in many other regions of the world (Figure 14.6). Because variations in pressure are associated with winds and rainfall, they were wanted to find out if pressure in one region could be used to forecast weather in other regions using the correlations.

The early studies found that the two strongest centers of the variability are near Darwin, Australia and Tahiti. The fluctuations at Darwin are opposite those at Tahiti, and resemble an oscillation. Furthermore, the two centers had strong correlations with pressure in areas far from the Pacific. Walker named the fluctuations the *Southern Oscillation*.

The *Southern Oscillation Index* is sea-level pressure at Tahiti minus sea-level pressure at Darwin (Figure 14.7). Usually, the index is normalized by the standard deviation. The index indicates the strength of the trade winds. When the index is high, the pressure gradient between east and west in the tropical Pacific is large, and the trade winds are strong. When the index is negative, trades, are weak.

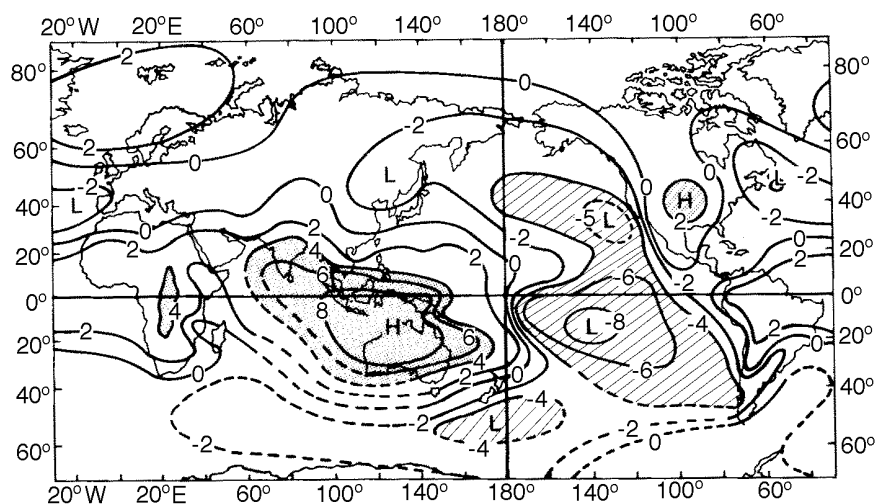


Figure 14.6 Correlation coefficient of annual-mean sea-level pressure with pressure at Darwin. - - - - Coefficient < -0.4 . (From Trenberth and Shea, 1987).

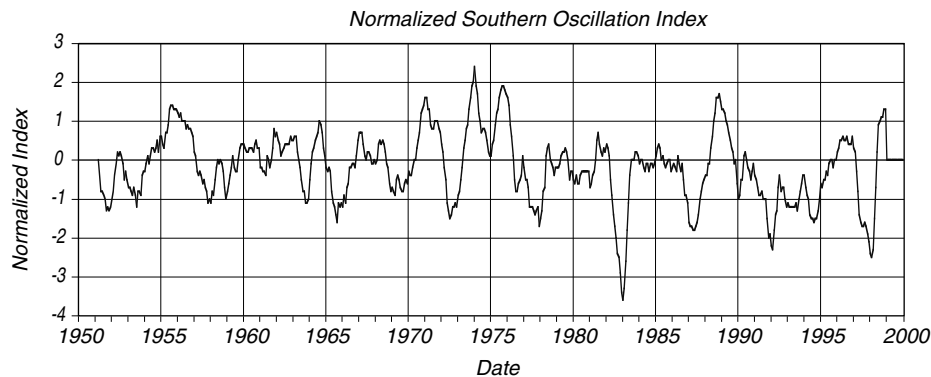


Figure 14.7 Normalized Southern Oscillation Index from 1951 to 1999. The normalized index is sea-level pressure anomaly at Tahiti divided by its standard deviation minus sea-level pressure anomaly at Darwin divided by its standard deviation then the difference is divided by the standard deviation of the difference. The means are calculated from 1951 to 1980. Monthly values of the index have been smoothed with a 5-month running mean. Strong El Niño events occurred in 1957–58, 1965–66, 1972–73, 1982–83, 1997–98. Data from NOAA.

The connection between the Southern Oscillation and El Niño was made soon after the Rancho Sante Fe meeting. Ichiye and Petersen (1963) and Bjerknes (1966) noticed the relationship between equatorial temperatures in the Pacific during the 1957 El Niño and fluctuations in the trade winds associated with the Southern Oscillation. The theory was further developed by Wyrтки (1975).

Because El Niño and the Southern Oscillation are so closely related, the phenomenon is often referred to as the *El Niño–Southern Oscillation* or ENSO. More recently, the oscillation is referred to as El Niño/La Niña, where La Niña refers to the positive phase of the oscillation when trade winds are strong, and water temperature in the eastern equatorial region is very cold.

Philander (1990) pointed out that each El Niño is unique, with different temperature, pressure, and rainfall patterns. Some are strong, others are weak. So, exactly what events deserve to be called El Niño? Recent studies based on the COADS data show that the best indicator of El Niño is sea-level pressure anomaly in the eastern equatorial Pacific from 4°S to 4°N and from 108°W to 98°W (Harrison and Larkin, 1998). It correlates better with sea-surface temperature in the central Pacific than with the Southern-Oscillation Index. Thus the importance of the El Niño is not exactly proportional to the Southern Oscillation Index—the strong El Niño of 1957–58, has a weaker signal in Figure 7 than the weaker El Niño of 1965–66.

Trenberth (1997), based on discussions within the Climate Variability and Predictability program, recommends that those disruptions of the equatorial system in the Pacific shall be called an El Niño only when the 5-month running mean of sea-surface temperature anomalies in the region 5°N – 5°S , 120°W – 170°W exceeds 0.4°C for six months or longer.

So El Niño, which started life as a change in currents off Peru each Christmas, has grown into a giant. It now means a disruption of the ocean-atmosphere system over the whole equatorial Pacific.

Theory of El Niño Wyrтки (1975) gives a clear, modern description of El Niño.

During the two years preceding El Niño, excessively strong southeast trades are present in the central Pacific. These strong southeast trades intensify the subtropical gyre of the South Pacific, strengthen the South Equatorial Current, and increase the east-west slope of sea level by building up water in the western equatorial Pacific. As soon as the wind stress in the central Pacific relaxes, the accumulated water flows eastward, probably in the form of an equatorial Kelvin wave. This wave leads to the accumulation of warm water off Ecuador and Peru and to a depression of the usually shallow thermocline. In total, El Niño is the result of the response of the equatorial Pacific to atmospheric forcing by the trade winds.

Sometimes the trades in the western Pacific not only weaken, they actually reverse direction for a few weeks to a month, producing *westerly wind bursts* that quickly deepen the thermocline there. The deepening of the thermocline launches an eastward propagating Kelvin wave and a westward propagating Rossby wave. (If you are asking, What are Kelvin and Rossby waves? I will answer that in a minute. So please be patient.)

The Kelvin wave deepens the thermocline as it moves eastward, and it carries warm water eastward. Both processes cause a deepening of the mixed layer in the eastern equatorial Pacific a few months after the wave is launched in the western Pacific. The deeper thermocline in the east shuts off the upwelling of cold water, and the surface temperatures offshore of Ecuador and Peru warm by 2–4°. The warm water reduces the temperature contrast between east and west, further reducing the trades and hastening the development of El Niño.

With time, the warm pool spreads east, eventually extending as far as 140°E (Figure 14.8). Plus, water warms in the east along the equator due to reduced upwelling, and to reduced advection of cold water from the east due to weaker trade winds.

The warm waters along the equator in the east cause the areas of heavy rain to move eastward from Melanesia and Fiji to the central Pacific. Essentially, a major source of heat for the atmospheric circulation moves from the west to the central Pacific, and the whole atmosphere responds to the change. Bjerkness (1972), describing the interaction between the ocean and the atmosphere over the eastern equatorial Pacific concluded:

In the cold ocean case (1964) the atmosphere has a pronounced stable layer between 900 and 800 mb, preventing convection and rainfall, and in the warm case (1965) the heat supply from the ocean eliminates the atmospheric stability and activates rainfall. . . . A side effect of the widespread warming of the tropical belt of the atmosphere shows up in the increase of exchange of angular momentum with the neighboring subtropical belt, whereby the subtropical westerly jet strengthens . . . The variability of the heat and moisture supply to the global atmospheric thermal engine from the equatorial Pacific can be shown to have far-reaching large-scale effects.

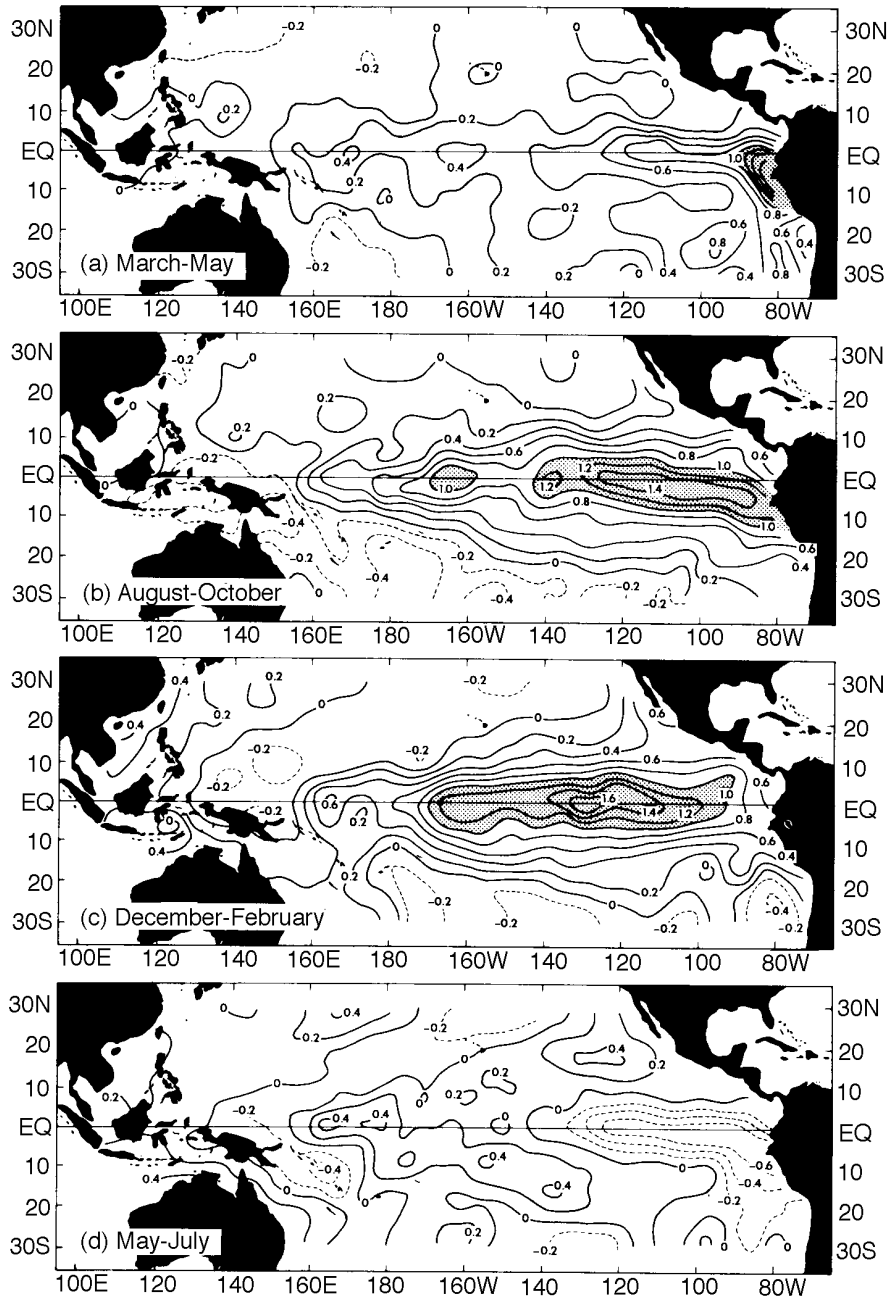


Figure 14.8 Anomalies of sea-surface temperature (in $^{\circ}\text{C}$) during a typical El Niño obtained by averaging data from El Niños between 1950 and 1973. Months are after the onset of the event. (From Rasmusson and Carpenter, 1982).

It is these far reaching events that make El Niño so important. Few people care about warm water off Peru around Christmas, many care about global changes the weather. El Niño is important because of its influence on the atmosphere.

After the Kelvin wave reaches the coast of Ecuador, part is reflected as an westward propagating Rossby wave, and part propagates north and south as a coastally trapped Kelvin wave carrying warm water to higher latitudes. For example, during the 1957 El Niño, the northward propagating Kelvin wave produced unusually warm water off shore of California, and it eventually reached Alaska. This warming of the west coast of North America further influences climate in North America, especially in California.

As the Kelvin wave moves along the coast, it forces other Rossby waves which move west across the Pacific with a velocity that depends on the latitude (14.4). The velocity is very slow at mid to high latitudes and fastest on the equator. There the reflected wave moves back as a deepening of the thermocline, reaching the central Pacific a year later. In a similar way, the westward propagating Rossby wave launched at the start of the El Niño in the west, reflects off Asia and returns to the central Pacific as a Kelvin wave, again about a year later.

El Niño ends when the Rossby waves reflected from Asia and Ecuador meet in the central Pacific about a year after the onset of El Niño (Picaut, Masia, and du Penhoat, 1997). The waves push the warm pool at the surface toward the west. At the same time, the Rossby wave reflected from the western boundary causes the thermocline in the central Pacific to become shallower when the waves reaches the central Pacific. Then any strengthening of the trades causes upwelling of cold water in the east, which increases the east-west temperature gradient, which increases the trades, which increases the upwelling (Takayabu et al 1999). The system is then thrown into the La Niña state with strong trades, and a very cold tongue along the equator in the east.

La Niña tends to last longer than El Niño, and the full cycle from La Niña to El Niño and back takes around three years. The cycle is not exact and El Niño comes back at intervals from 2-7 years, with an average near four years (Figuer 14.7).

Equatorial Kelvin and Rossby Waves Kelvin and Rossby waves are the ocean's way of adjusting to changes in forcing such as westerly wind bursts. The adjustment occurs as waves of current and sea level that are influenced by gravity, Coriolis force f , and the north-south variation of Coriolis force $\partial f / \partial y = \beta$. There are many kinds of these waves with different spatial distributions, frequencies, wavelengths, speed and direction of propagation. If gravity and f are the restoring forces, the waves are called Kelvin and Poincare waves. If β is the restoring force, the waves are called planetary waves. One important type of planetary wave is the Rossby wave.

Two types of waves are especially important for El Niño: internal Kelvin waves and Rossby waves. Both waves can have modes that are confined to a narrow, north-south region centered on the equator. These are *equatorially trapped waves*. Both exist in slightly different forms at higher latitudes.

Kelvin and Rossby wave theory is beyond the scope of this book, so I will

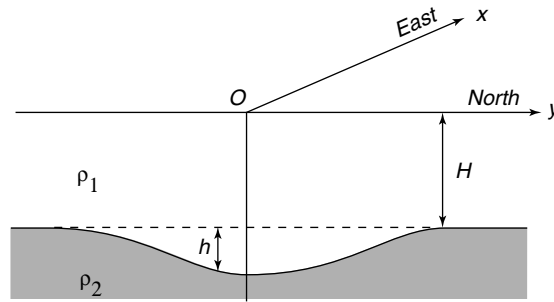


Figure 14.9 Sketch of the two-layer model of the equatorial ocean used to calculate planetary waves in those regions (From Philander, 1990).

just tell you what they are without deriving the properties of the waves. If you are curious, you can find the details in Philander (1990): Chapter 3; Pedlosky (1987): Chapter 3; and Apel (1987): §6.10–6.12. If you know little about waves, their wavelength, frequency, group and phase velocities, skip to Chapter 16 and read §16.1.

The theory for equatorial waves is based on a simple, two-layer model of the ocean (Figure 14.9). Because the tropical oceans have a thin, warm, surface layer above a sharp thermocline, such a model is a good approximation for those regions.

Equatorial-trapped Kelvin waves are non-dispersive, with group velocity:

$$c_{Kg} = c \equiv \sqrt{g'H}; \quad \text{where} \quad g' = \frac{\rho_2 - \rho_1}{\rho_1} g \quad (14.2)$$

g' is reduced gravity, ρ_1, ρ_2 are the densities above and below the thermocline, and g is gravity. Trapped Kelvin waves propagate only to the east. Note, that c is the phase and group velocity of a shallow-water, internal, gravity wave. It is the maximum velocity at which disturbances can travel along the thermocline.

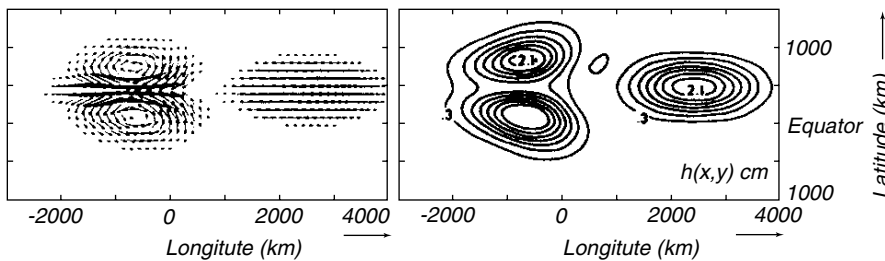


Figure 14.10 **Left:** Horizontal currents associated with equatorially trapped waves generated by a bell-shaped displacement of the thermocline. **Right:** Displacement of the thermocline due to the waves. The figures shows that after 20 days, the initial disturbance has separated into an westward propagating Rossby wave (left) and an eastward propagating Kelvin wave (right). (From Philander et al. 1984).

Typical values of the quantities in (14.2) are:

$$\frac{\rho_2 - \rho_1}{\rho_1} = 0.003; \quad H = 150 \text{ m}; \quad c = 2.1 \text{ m/s}$$

At the equator, Kelvin waves propagate eastward at speeds of up to 3 m/s, and they cross the Pacific in a few months. Currents associated with the wave are everywhere eastward with north-south component (Figure 14.10).

Kelvin waves can also propagate poleward as a trapped wave along an east coast of an ocean basin. Their group velocity is also given by (14.3), and they are confined to a coastal zone with width $x = c/(\beta y)$

The important Rossby waves on the equator have frequencies much less than the Coriolis frequency. They can travel only to the west. The group velocity is:

$$c_{Rg} = -\frac{c}{(2n+1)}; \quad n = 1, 2, 3, \dots \quad (14.3)$$

The fastest wave travels westward at a velocity near 0.8 m/s. The currents associated with the wave are almost in geostrophic balance in two counter-rotating eddies centered on the equator (Figure 14.10).

Away from the equator, low-frequency, long-wavelength Rossby waves also travel only to the west, and the currents associated with the waves are again almost in geostrophic balance. Group velocity depends strongly on latitude:

$$c_{Rg} = -\frac{\beta g' H}{f^2} \quad (14.4)$$

The wave dynamics in the equatorial regions differ markedly from wave dynamics at mid-latitudes. The baroclinic waves are much faster, and the response of the ocean to changes in wind forcing is also much faster than at mid-latitudes.

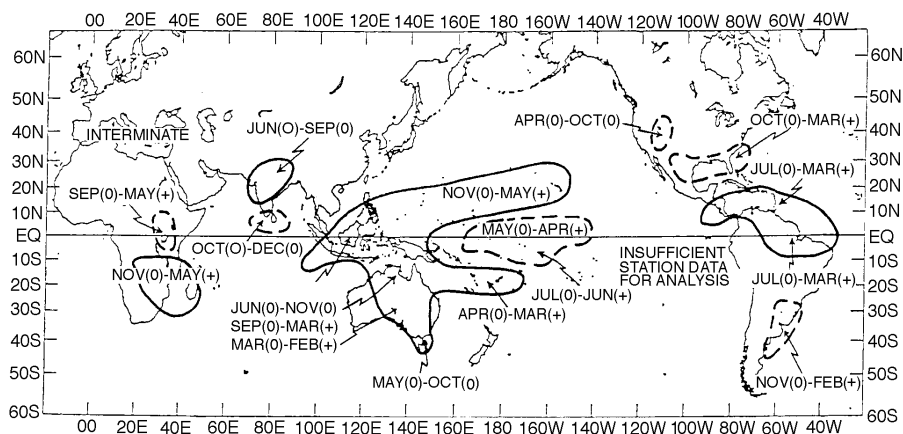


Figure 14.11 Sketch of regions receiving enhanced rain (dashed lines) or drought (solid lines) during an El Niño event. (0) indicates that rain changed during the year in which El Niño began, (+) indicates that rain changed during the year after El Niño began. (From Ropelewski and Halpert, 1987).

For the planetary waves confined to the equator, we can speak of an *equatorial wave guide*.

Now, let's return to El Niño and its "far-reaching large-scale effects."

14.3 El Niño Teleconnections

Teleconnections are statistically significant correlations between weather events that occur at different places on the Earth. Figure 14.11 shows the dominant global teleconnections associated with the El Niño/Southern Oscillation ENSO. It shows that ENSO is an atmospheric perturbation influencing the entire Pacific.

The influence of ENSO is through its influence on convection in the equatorial Pacific. As the area of heavy rain moves east, it perturbs atmospheric pressure (Figure 14.12) and influences the position of the jet stream at higher latitudes. This sequence of events leads to some predictability of weather patterns a season in advance over North America, Brazil, Australia, South Africa and other regions.

The ENSO perturbations to mid-latitude and tropical weather systems leads to dramatic changes in rainfall in some regions (Figure 14.12). As the convective regions migrate east along the equator, they bring rain to the normally arid, central-Pacific islands. The lack of rain in the western Pacific leads to drought in Indonesia and Australia.

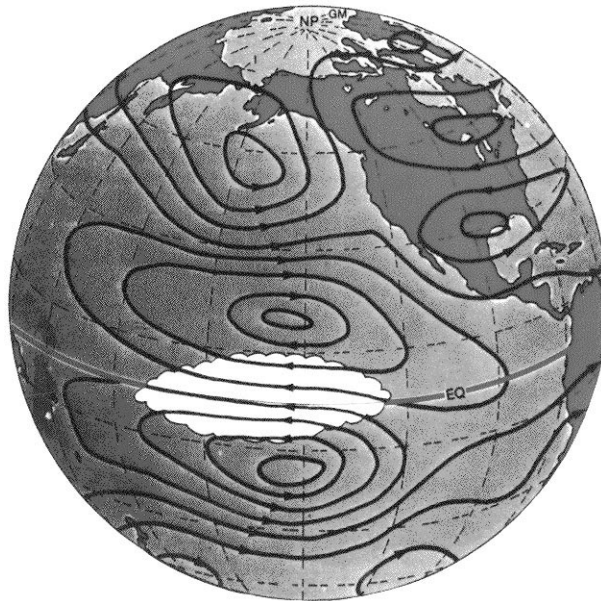


Figure 14.12 Changing patterns of convection in the equatorial Pacific during an El Niño, set up a pattern of pressure anomalies in the atmosphere (solid lines) which influence the extratropical atmosphere. (From Rasmusson and Wallace, 1983).

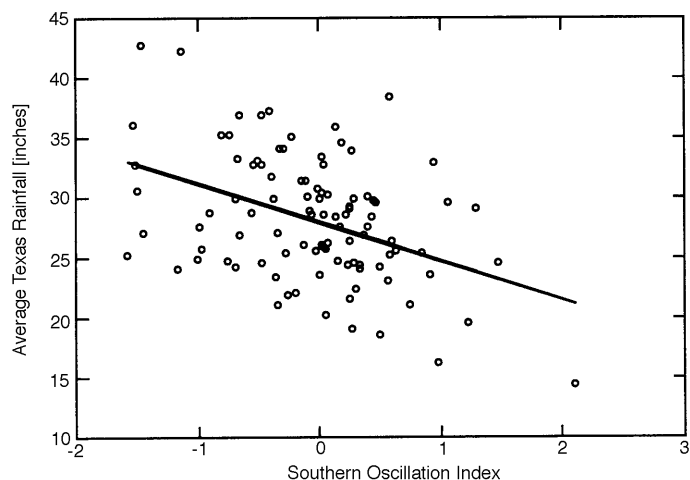


Figure 14.13 Correlation of yearly averaged rainfall averaged over all Texas each year plotted as a function of the Southern Oscillation Index averaged for the year. (From Stewart, 1994).

An Example: Variability of Texas Rainfall Figure 14.11 shows a global view of teleconnections. Let's zoom in to one region, Texas, that I chose only because I live there. The global figure shows that the region should have higher than normal rainfall in the winter season after El Niño begins. I therefore correlated yearly averaged rainfall for the state of Texas to the Southern Oscillation Index; and I found that the rainfall is well correlated (Figure 14.13). Wet years correspond to El Niño years in the equatorial Pacific. During El Niño, convection normally found in the western equatorial Pacific moved east into the central equatorial Pacific. The subtropical jet also moves east, carrying tropical moisture across Mexico to Texas and the Mississippi Valley. Cold fronts in winter interact with the upper level moisture to produce abundant winter rains from Texas eastward.

14.4 Observing El Niño

The tropical and equatorial Pacific is a vast, remote area seldom visited by ships. To observe the region NOAA's Pacific Marine Environmental Laboratory has deployed an array of buoys to measure oceanographic and meteorological variables (Figure 14.14). The first buoy was successfully deployed in 1976 by David Halpern. Since that simple start, new moorings have been added to the array, new instruments have been added to the moorings, and the moorings have been improved. The program has now evolved into the Tropical Atmosphere Ocean TAO array of approximately 70 deep-ocean moorings spanning the equatorial Pacific Ocean between 8°N and 8°S from 95°W to 137°E.

The array began full operation in December 1994, and it continues to evolve. The work necessary to design and calibrate instruments, deploy moorings, and process data is coordinated through the TAO Project. It is a multi-national effort involving the participation of the United States, Japan, Korea, Taiwan,

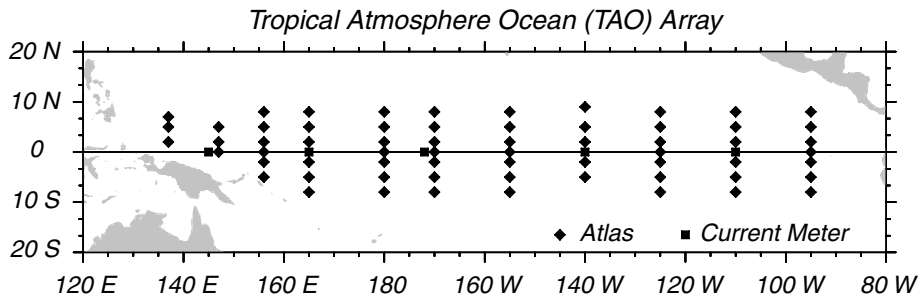


Figure 14.14 Tropical Atmosphere Ocean TAO array of moored buoys operated by the NOAA Pacific Marine Environmental Laboratory with help from Japan, Korea, Taiwan, and France.

and France with a project office at the Pacific Marine Environmental Laboratory in Seattle, Washington.

The TAO moorings measure air temperature, relative humidity, surface wind velocity, sea-surface temperatures, and subsurface temperatures from 10 meters down to 500 meters. Five moorings located on the equator at 110°W , 140°W , 170°W , 165°E , and 147°E also carry upward-looking Acoustic Doppler Current Profilers ADCP to measure upper-ocean currents between 10 m and 250 m. The moorings are designed to last about a year, and moorings are recovered and replaced yearly. Data from the array are sent back through ARGOS system, and data are processed and made available in near real time. All sensors are calibrated prior to deployment and after recovery.

Data from TAO are being supplemented with data from tide gauges and satellites. Sea level is measured by approximately 80 tide gauges operated by the Integrated Global Observing System. The gauges are located on more than 30 small islands and at 40 shore stations throughout the Pacific. Data from the stations are relayed to shore via satellites, processed, and made available in near real time. Altimeters on Topex/Poseidon and ERS-1 observe the ocean's topography between the island stations and across the deep ocean.

The Topex/Poseidon observations are especially useful. They provided detailed views of the development of the 1997–1998 El Niño in near real time that were widely reproduced throughout the world. The satellite data extended beyond the TAO data to include the entire tropical Pacific, producing maps of sea level every ten days. Animations of the maps show the Kelvin waves crossing the Pacific, and extending along the coasts of the Americas.

Rain rates are measured by NASA's Tropical Rainfall Measuring Mission which was specially designed to observe rain rates. It was launched on 27 November 1997, and it carries five instruments: the first spaceborne precipitation radar, a five-frequency microwave radiometer, a visible and infrared scanner, a cloud and earth radiant energy system, and a lightning imaging sensor. Working together, the instruments provide data necessary to produce monthly maps of tropical rainfall averaged over 500 km by 500 km areas with 15% accuracy. The grid is global between $\pm 35^{\circ}$ latitude. In addition, the satellite data are used to measure latent heat released to the atmosphere by rain, thus providing continuous monitoring of heating of the atmosphere in the tropics.

Further information about processes in the western Pacific warm pool were obtained through a very large, international, Coupled Ocean Atmosphere Response Experiment COARE 1992–1994. During the intensive observing period of the experiment from 1 November 1992 to 28 February 1993, instruments on dozens of moorings, ships, islands, aircraft, and satellites observed the region bounded by 30°N, 30°S, 130°W, and 90°E. The goal was to obtain a better understanding of processes over the warm pool, the TOGA-COARE domain, especially heat fluxes from the ocean during weak winds, the organization of the convection in the atmospheric, the ocean’s response to the forcing, and the interactions that extend the oceanic and atmospheric influence of the warm pool system to other regions and vice versa. Results from the experiment are beginning to influence the development of numerical models for predicting El Niño.

14.5 Forecasting El Niño

The importance of El Niño to global weather patterns has led to many schemes for forecasting events in the equatorial Pacific. Several generations of models have been produced, but the skill of the forecasts has not always increased. Some models worked well for a few years, then failed. Failure was followed by improved models, and the cycle continued. Thus, the best models in 1991 failed to predict two warm events (weak El Niños) in 1993 and 1994 (Ji, Leetmaa, and Kousky, 1996); and the best model of the 1980s failed to predict the onset of the strong El Niño of 1997–1998 although the onset was predicted by a new model developed by the National Centers for Environmental Prediction. In general, the more sophisticated the model, the better the forecasts (Kerr, 1998). The best predictions of the 1997/1998 El Niño came from the U.S. National Centers for Environmental Prediction and the European Center for Medium-Range Weather Forecasts.

The following recounts some of the more recent work to improve the forecasts. For simplicity, I describe the technique used by the National Centers for Environmental Prediction (Ji, Behringer, and Leetmaa, 1998); but Chen et al. (1995), Latif et al. (1993), and Barnett et al. (1993), among others, have all developed useful prediction models.

Atmospheric Models Our ability to understand El Niño depends in part on our ability to model the atmospheric circulation in the equatorial Pacific. How well then do we know atmospheric processes over the Pacific?

To help answer the question, the World Climate Research Program has sponsored a program to intercompare the output from 30 different numerical models of the atmosphere during the period 1979–1988, the Atmospheric Model Intercomparison Project (Gates, 1992). The subproject on *The Variability in the Tropics: Synoptic to Intraseasonal Timescales* is especially important (Slingo et al. 1995) because it documents the ability of 15 atmospheric general-circulation models to simulate the observed variability in the tropical atmosphere. The models included several operated by government weather forecasting centers, including the model used for day-to-day forecasts by the European Center for Medium-Range Weather Forecasts.

The first results of the tropical study indicate that none of the models were able to duplicate all important interseasonal variability of the tropical atmosphere. The intraseasonal variability includes timescales of 2 to 80 days. The results also show that models with weak intraseasonal activity tend to also have a weak annual cycle. Most models seemed to simulate some important aspects of the interannual variability including El Niño. The length of the time series was, however, too short to provide conclusive results on interannual variability.

The results of the substudy imply that numerical models of the atmospheric general circulation need to be improved if they are to be used to study tropical variability and the response of the atmosphere to changes in the tropical ocean. Some of the improvement is coming from new knowledge gained from COARE.

Oceanic Models Our ability to understand El Niño also depends in part on our ability to model the oceanic circulation in the equatorial Pacific. Because the models provide the initial conditions used for the forecasts, they must be able to assimilate up-to-date measurements of the Pacific along with heat fluxes and surface winds calculated from the atmospheric models. The measurements could include sea-surface winds from scatterometers and moored buoys, surface temperature from the optimal-interpolation data set (see §6.6), subsurface temperatures from buoys and XBTs, and sea level from altimetry and tide-gauges on islands.

Ji, Behringer, and Leetmaa (1998) at the National Centers for Environmental Prediction have modified the Geophysical Fluid Dynamics Laboratory's Modular Ocean Model for use in the tropical Pacific (see §15.4 for more information about this model). Its domain is the Pacific between 45°S and 55°N and between 120°E and 70°W. The zonal resolution is 1.5°. The meridional resolution is 1/3° within 10° of the equator, increasing smoothly to 1° poleward of 20° latitude. It has 28 vertical levels, with 18 in the upper 400 m to resolve the mixed layer and thermocline. The model is driven by mean winds from Hellerman and Rosenstein (1983), anomalies in the wind field from Florida State University, and mean heat fluxes from Oberhuber (1988). It assimilates subsurface temperature from the TAO array and XBTs, and surface temperatures from the monthly optimal-interpolation data set (Reynolds and Smith, 1994).

The output of the this model is an ocean analysis, the density and current field that best fits the data used in the analysis. This is used to drive a coupled ocean-atmosphere model to produce forecasts. Figure 14.3 is an example of the currents calculated by the model.

Coupled Models As the name implies, coupled models are separate atmospheric and oceanic models that pass information through their common boundary at the sea surface, thus coupling the two calculations. The coupling can be one way, from the atmosphere, or two way, into and out of the ocean. In the scheme used by the NOAA National Centers for Environmental Prediction the ocean model is the same Modular Ocean Model described above. It is coupled to a low-resolution version of the global, medium-range forecast model operated by the National Centers (Ji, Kumar, and Leetmaa, 1994). Anomalies of wind stress, heat, and fresh-water fluxes calculated from the atmospheric model are added to the mean annual values of the fluxes, and the sums are used

to drive the ocean model. Sea-surface temperature calculated from the ocean model is used to drive the atmospheric model from 15°N to 15°S .

As computer power decreases in cost, the models are becoming ever more complex. The trend is to global coupled models able to include other coupled ocean-atmosphere systems in addition to ENSO. We return to the problem in §15.7 where I describe global coupled models.

Forecasts In general, the coupled ocean-atmosphere models produce the best forecasts. The forecasts include not only events in the Pacific but also the global consequences of El Niño. The forecasts are judged two ways:

1. Using the correlation between the area-averaged sea-surface-temperature anomalies from the model and the observed temperature anomalies in the eastern equatorial Pacific. The area is usually from 170°W to 120°W between 5°S and 5°N . Useful forecasts have correlations exceeding 0.6.
2. Using the root-mean-square difference between the observed and predicted sea-surface temperature in the same area.

Forecasts made from the National-Centers coupled model had correlations that exceeded 0.6 as far as one year in advance when run using data from 1981 to 1995. The root-mean-square difference in temperature was less than 1°C for the forecasts. Forecasts had less skill for the period from 1992 to 1995, the period with weak warming events that have proved difficult to forecast. During that period, correlations exceed 0.6 for only eight months, although the temperature error was less than 0.7°C . The most accurate forecasts were those that started during the northern hemisphere warm period from May through September. Forecasts made in November through January were significantly less accurate (Ji, Behringer, and Leetmaa, 1998).

In conclusion, it appears that coupled ocean-atmosphere models driven with accurate atmospheric and oceanic data can produce useful forecasts of El Niño.

14.6 Important Concepts

1. Equatorial processes are important because heat released by rain in the equatorial region drives an important part of the atmospheric circulation.
2. Equatorial currents redistribute heat; and interannual variability of currents and temperatures in the equatorial Pacific modulates the oceanic forcing of the atmosphere.
3. Changes in equatorial dynamics cause changes in atmospheric circulation.
4. El Niño causes the biggest changes in equatorial dynamics. During El Niño, trade-winds weaken in the western Pacific, the thermocline becomes less deep in the west. This drives a Kelvin wave eastward along the equator, which deepens the thermocline in the eastern Pacific. The warm pool in the west moves eastward toward the central Pacific, and the intense tropical rain areas move with the warm pool.
5. As a result of El Niño, drought occurs in the Indonesian area and northern Australia, and floods occur in western, tropical South America. Variations

in the atmospheric circulation influence more distant areas through teleconnections.

6. Forecasts of El Niño are made using coupled ocean-atmospheric numerical models. Forecasts appear to have useful accuracy for 6–12 months in advance.